Mimusops elengi Seed Shell Powder as a New Bio-Filler for Polypropylene-based Bio-Composites

Mathialagan Muniyadi,[a,*] Tiffany Yit Siew Ng,[a] Yamuna Munusamy,[a] and Zhong Xian Ooi [b]

Mimusops elengi seed shell powder (MESSP) was introduced as a new bio-filler in polypropylene (PP). The MESSP was characterized using a particle size analyzer, scanning electron microscopy (SEM), Fourier transform infrared spectroscopy, and a thermogravimetric analyzer. MESSP was successfully melt mixed with polypropylene to produce bio-composite at various MESSP loading. The processability and properties of the bio-composites were characterized by using processing torques, differential scanning calorimetry, tensile test, water absorption, and SEM. The processability of PP was not affected by the addition of MESSP, which was revealed from the minimum changes in the processing torques, melting temperature, crystallization temperature, and degree of crystallinity. The tensile strength and elastic modulus of the bio-composites were improved with an addition of MESSP of up to 10 wt.%. However, the elongation at break and resistance to water absorption decreased slightly with increased MESSP loading. Morphological observations revealed that the MESSP showed good dispersion and adhesion in the PP matrix of up to 5 wt.% MESSP. Above 5 wt.% MESSP, agglomerates formed, which influenced the physical-mechanical properties of the PP and MESSP bio-composites. Results indicated that PP/MESSP composites can be used to replace PP in applications such as car dashboards and door panel, furniture, and rigid packaging.

Keywords: Bio-composites; Mimusops elengi; Polypropylene; Tensile test; Water absorption; Scanning electron microscope

Contact information: a: Department of Petrochemical Engineering, Faculty of Engineering and Green Technology, Universiti Tunku Abdul Rahman, Jalan Universiti, Bandar Barat, 31900 Kampar, Perak, Malaysia; b; Department of Chemical Science, Faculty of Science, Universiti Tunku Abdul Rahman, Jalan Universiti, Bandar Barat, 31900 Kampar, Perak, Malaysia;
**Corresponding author: mathialagan@utar.edu.my.*

INTRODUCTION

The diversity in processing, highly specific stiffness, and high economic value of bio-fillers have attracted many researchers and manufacturers in developing new bio-composites (Faruk *et al.* 2012). According to Prnewswire (2015), 3.9% compound annual growth is expected in the global polymer industry from the year 2015 to 2020. Polymeric materials are progressively replacing metals, paper, glass, and other traditional materials in various applications due to their lightweight properties, wide range in strength, flexibility in design, and low cost. However, with the gradual increase in demand, the production and consumption of polymer based products has resulted in a high dependency on fossil fuels and has increased the amount of polymer waste (Hamad *et al*. 2013). Furthermore, the inappropriate disposal of polymer products has released pollution

effluents and toxic intermediates to the surrounding areas, which is hazardous to humans and the environment (Stein 2002).

Polymer wastes are generally disposed of through landfilling, which may take thousands of years to be completely decomposed due to its non-biodegradable nature. Polymer wastes are also recycled into new products or incinerated to generate energy. However, recycling and incineration are not completed at commercial scale due to high production costs and the possibility of dissipating hazardous gases into the environment. Thus, producing a bio-degradable polymer is the most suitable alternative to efficiently manage polymer waste. An increase in the utilization of bio-plastics can decrease the carbon footprint, greenhouse gas emissions, and pollution risks from polymer consumption. Thus, the development of new bio-fillers for polymers could improve the bio-degradability and shorten the landfill life (Faruk *et al*. 2012; Stein 2002).

The major issues of material availability and environmental sustainability have led to the introduction of natural fillers, also known as bio-fillers, into polymer matrices to produce bio-composites (Faruk *et al*. 2012). Bio-composites have been developed with natural fillers such as kenaf, jute, sisal, hemp, areca, bamboo, palm, and cotton (Sathishkumar *et al*. 2014). For instance, kenaf fibers are a commercially available natural filler that can be used in polypropylene to produce composites for automotive parts; kenaf fibers are lighter in weight and can be easily disposed of (Shibata *et al.* 2006). However, the properties of bio-composites are generally low due to incompatibility between the hydrophilic bio-fillers and hydrophobic polymers. The addition of bio-fillers also decreases the thermal stability and resistance to water absorption (Fakhrul and Islam 2013; Alomayri *et al*. 2014).

Mimusops elengi (*M. elengi*) is a tree native to the western peninsular region of South India. It belongs to the Sapotaceae family and is popularly known as Spanish cherry, medlar, and bullet wood in English. This plant is a small to large evergreen ornamental tree planted along road sides and residential areas and can grow up to 16 meters in height. The tree grows in other parts of India, Burma, Pakistan, Thailand, and Malaysia (Mitra 1981; Boonyuen *et al*. 2009; Baliga *et al*. 2011). The bark, fruit, and seeds of *M. elengi* are used in traditional medicine (Gami *et al*. 2012). *M. elengi* bark contains tannin, caoutchouc, wax, starch, and ash, whereas the flowers contain volatile oils. The seeds contain a fixed amount of fatty oil (Kadam *et al*. 2012; Lim 2013). Current research has utilized *M. elengi* fruits and kernels to produce biodiesel (Bora *et al.* 2014; Dutta and Deka 2014).

M. elengi fruits are edible and are used to produce cooking oils. However, its high alkaloid content makes it less popular than oil from other sources, such as sunflower and peanut. The bio-fillers currently used in polymer composites are cultivated at specific plantations, which requires a large area. As the fruits and seeds of *M. elengi* are underutilized and it requires no additional plantation area to grow, it is potentially a good source of bio-filler in bio-composites. While no previous research has utilized *M. elengi* as filler in polymer composites, *M. elengi* is gaining more attention in biomass and bio-diesel production, which will allow the exploitation of *M. elengi* in various fields in the future.

This work produced polypropylene based bio-composites using *M. elengi* seed shell powder (MESSP) as a new bio-filler. The effects of various MESSP loading on the processability, tensile properties, water absorption, and morphological properties of PP and MESSP bio-composites were investigated.

EXPERIMENTAL

Materials

The polymeric matrix used in this study was polypropylene (PP), and it was supplied by Lotte Chemical Titan (Pasir Gudang, Johor, Malaysia) under the trade name Titanpro; it is a type of polypropylene homopolymer. The product grade was Titanpro® PD943, and it is used to produce bags for hosiery, shirts, textiles, and food packaging and to manufacture plastic articles through extrusion, molding, or other conversion processes. The chemical abstract service (CAS) registry number is 9003-07-0. The density of PP is 0.9 g/cm^{-3}, and it has a melt flow rate of 1.1g/min. The melting point of PP is 160 °C, and it is available as solid pellets ranging from translucent to white.

The *M. elengi* seed shell powder (MESSP) filler was produced from the seeds of *M. elengi* (ME) plants (Taman Kampar Perdana, Kampar, Perak, Malaysia). The seeds were collected by gently squeezing ripe ME fruits, which varied from an orange to reddish color. The seeds were dried daily under sunlight for 4 h to 5 h for one week. The kernel was then removed by breaking the seed to obtain the dried seed shell. The dried seed shells were cleaned with distilled water by stirring at 300 rpm using a magnetic stirrer at 80 °C for 2 h. The ratio of the seed shell to distilled water was at least 1:3 by volume. The cleaned seed shells were tossed using a sieve and oven-dried (Memmert, Schwabach, Germany) at 80 °C for 24 h, followed by grinding (RT-08 grinder machine, Mill Powder Tech Solutions, Tainan city, Taiwan). The grinding was done in batches of maximum 350 g of ME seeds with a limit of 30 s to 45 s of grinding at a time. Finally, the crushed seed shells were sieved to less than 45 µm particle size using a W.S. Tyler® Ro-Tap® sieve shaker (RX-29-10, Hogentogler & Co. Inc, Columbia, MD, USA) to obtain MESSP.

Bio-composites preparation

PP pellets and MESSP were pre-dried in oven at 80 °C for 24 h to expel any absorbed moisture. A calculated amount of PP and MESSP was prepared according to the compounding formulation shown in Table 1. PP pellets and MESSP were pre-mixed in a beaker prior to discharge into the mixer, and the total mass of the compound was 45 g. Bio-composite compounds containing various ratios of MESSP were then prepared by melt mixing of PP and MESSP using a Brabender internal mixer (Plastograph® EC815652, Duisburg, Germany) at a processing temperature of 180 °C, a mixing time of 10 min, and a mixing speed of 60 rpm. The compounds were compressed into sheets with a thickness of 1 mm using a hydraulic hot and cold press machine (GT-7014-A30C, GOTECH Testing Machines Inc., Taichung City, Taiwan). The compression process was carried out at 180 °C, with preheating, hot pressing, and cool pressing time of 12, 4, and 2 min, respectively.

Table 1. Compounding Formulation of PP/MESSP Bio-composites

Sample Code	Composition (wt.%)	
	PP	MESSP
PP/MESSP-0%	100	0
PP/MESSP-1%	99.0	1.0
PP/MESSP-2.5%	97.5	2.5
PP/MESSP-5%	95.0	5.0
PP/MESSP-10%	90.0	10.0

Methods

Characterization of MESSP and PP/MESSP bio-composites

The refractive index of MESSP was measured using a digital refractometer (300034, Sper Scientific Ltd., Scottsdale, AZ, USA) prior to particle size analysis. Water was used as a dispersant, and the MESSP refractive index obtained was 1.3335. The mean particle size, particle size distribution, and specific surface area of MESSP was characterized with a Malvern Mastersizer particle size analyzer (Hydro 2000MU, Malvern Instrument Ltd, Malvern, UK).

The chemical functionality of the MESSP was characterized with a Fourier transform infrared (FTIR) spectrophotometer (Spectrum RX1, Perkin Elmer Inc., Norwalk, CT, USA) to better understand the possible interaction that can form between PP and MESSP. For MESSP characterization, the KBr pelletizing method was used to form the MESSP specimens for analysis. MESSP was pulverized and mixed with KBr using a mortar and pestle with a KBr and MESSP ratio of 10:1. The mixture was compressed on a pellet-forming die using a hydraulic press (International Crystal Laboratories, Garfield, NJ, USA). The formed pellet was oven-dried to remove moisture. The spectrum was scanned within 400 cm^{-1} to 4000 cm^{-1}, with 16 scans, a 4.0 cm^{-1} resolution, 1.0 cm^{-1} interval, and recorded in transmittance (%*T*).

The morphology of MESSP and PP/MESSP bio-composites were studied using a scanning electron microscope (JSM 6701-F, Jeol, Akishima, Japan) and conducted with an accelerating rate of 20.0 kV. For MESSP, the magnification of analysis was 500x and 1000x with a working distance of 8.1 mm. For PP/MESSP bio-composites, the analysis was carried out at 1000x magnification with a working distance ranging from 5.3 mm to 6.5 mm, depending on the focus point. Prior to analysis, the samples were sputter coated with a thin layer of platinum with an approximate thickness of 15 nm and density of 21.45 g/cm^{-3} using a sputtering machine (JFC-1600, Jeol, Akishima, Japan) to prevent electrostatic charging and poor resolution during the analysis.

The thermal decomposition of MESSP was characterized using a Mettler-Toledo thermal analyzer (TGA/SDTA851^{e}, Mettler-Toledo International Inc., Schwarzenbach, Switzerland). Approximately 4 mg to 5 mg of MESSP was weighed using a hermetically sealed aluminum crucible, placed inside a tube furnace, and heated from 30 °C to 600 °C with a heating rate of 20 °C/min under nitrogen with a flowrate of 50 mL/min using a recirculating cooler. The percentage weight loss *versus* temperature was plotted to determine the thermal decomposition temperature and thermal stability of MESSP.

Processability measurement of PP/MESSP bio-composites

The processability of PP/MESSP bio-composites was evaluated from the processing torque values generated during melt mixing in an internal mixer, and thermal characteristics such as the melting temperature, crystallization temperature, and degree of crystallinity were obtained from differential scanning calorimetry (DSC).

The processing torque, also known as the loading and stabilization torque, was recorded during the melt mixing of PP and MESSP using a Plastograph® EC Brabender internal mixer (815652, Duisburg, Germany) with a processing temperature of 180 °C, mixing time of 10 min, and mixing speed of 60 rpm. In polymer processing, torque values reveal the rheological properties of composites such as viscosity, processability, and stiffness (Aho 2011). Low and stable torque values indicate easy processing and low stiffness of the composites and homogeneous dispersion of filler in the polymer matrix (Viet *et al*. 2012).

The thermal characterization such as melting temperature (T_m), crystallization temperature (T_c), enthalpy of melting (ΔH_m), and degree of crystallinity (X_c^m) was evaluated by DSC analysis (Mettler-Toledo International Inc., Schwarzenbach, Switzerland). Approximately 7 mg to 8 mg of PP/MESSP bio-composites was weighed using a hermetically sealed aluminum crucible. The crucible was placed in the tube furnace and heated from 25 °C to 300 °C with a heating rate of 10 °C/min under nitrogen at a flowrate of 10 mL/min. The specimens were immediately cooled to 25 °C after the heating cycle to analyze the cooling behavior. The degree of crystallinity of the bio-composites was calculated using Eq. 1,

$$X_c^m = \frac{\Delta H_m}{W_p \, x \, \Delta H_{100}} x100\% \quad (1)$$

where X_c^m was the degree of crystallinity in percentage, ΔH_m was the enthalpy of melting of the sample (J/g), ΔH_{100} was the enthalpy of melting for 100% crystalline polypropylene was 207 J/g, and W_p was the weight fraction of PP in the bio-composite.

Water absorption measurement

The water absorption test was conducted in accordance with ASTM D570-98 (2010). The bio-composite samples were oven-dried at 80 °C for 2 h to remove any absorbed moisture prior to the test. The samples were labeled accordingly, and 5 samples were tested for each composite. The initial weight (W_i) of the samples was measured using an electronic analytical and precision balance (Sartorius M-Pact AX224, Sartorius AG, Germany) and recorded. The samples were immersed in different water bottles with the same amount of water. The samples were immersed in water for 72 h at 25 °C in a dark environment. After 72 h, the samples were removed and weighed to obtain the final weight (W_f). The percentage of water absorption (W_a) was calculated by Eq. 2. A high percentage of water absorption indicates low resistance of the bio-composites towards water absorption.

$$W_a = \frac{W_f - W_i}{W_i} x100\% \quad (2)$$

Tensile test

The tensile test was performed using a light-weight tensile tester (Tinius Olsen H10KS-0748, Salfords, UK) according to ASTM D638-14 (2014). The composite sheet was cut into dumbbell shape specimens using a dumbbell cutter (Leader Technology Scientific (M) Sdn. Bhd., Balakong, Malaysia). For each composition, 5 dumbbell shaped specimens were cut and labeled. The thickness of each specimen had an average thickness of 1.00 mm and was measured using digital thickness gages (Series 542 Flat Anvil type, Mitutoyo America Corporation, Kuala Lumpur, Malaysia). The film was subjected to a 450 N load cell, 1000 mm of extension range, with 26 mm of gauge length and a crosshead speed of 50 mm/min until the specimen fractured. All tests were conducted at room temperature, and the average values for the tensile strength, E-modulus, and elongation at the break of the 5 repeated specimens were summarized for each composition from the stress-strain curve.

RESULTS AND DISCUSSION

Characterization of *Mimusops Elengi* Seed Shell Powder

In the past, there has been no similar research work reported on the characterization and melt mixing of MESSP in polymer composites. Thus, the characteristics of MESSP such as average particle size, specific surface area, the particle size distribution, chemical surface functionality, particle shape, structure, morphology, and thermal stability were determined to elucidate the possible interaction between MESSP and PP matrix. The MESSP was characterized by particle size analysis (PSA), FTIR spectroscopy, SEM, and TGA.

Table 2 shows the physical properties of the MESSP such as the mean diameter, particle size distribution, and specific surface area as evaluated by particle size analysis. The knowledge of the physical properties of fillers such as the particle size distribution and mean diameter may be crucial in understanding the effect of adding fillers on the processability, thermal, and mechanical properties of the polymer composites (Lu and Xu 1997). The MESSP had a narrower particle size distribution of approximately 37.2 µm. According to Bjørk *et al.* (2012), filler materials that have a narrow particle size distribution may lead to a more uniform structure than those having a broader distribution. Smaller particles could lead to a better dispersion of the filler in the polymer matrix and facilitate the processability of the polymer composites.

The MESSP particles were smaller in diameter with a mean diameter of 0.583 µm, which suggests that the MESSP was well dispersed in the PP matrix. In addition, the MESSP had a high specific surface area of 21.9 m^2/g due to its small particle size. The specific surface area was defined as the total surface area exposed of a finely divided filler to interact with the polymer matrix (Bjørk *et al.* 2012). Thus, the higher the specific surface area of the MESSP indicated that there was more contact surface area available, with a higher potential to reinforce the PP composites.

Table 2. Physical Properties of MESSP

Characteristics	Values
Particle Size Distribution (µm)	0.04 – 37.24
Distribution Range (µm)	37.20 ± 0.04
Mean Diameter (µm)	0.583 ± 0.011
Specific Surface Area (m^2/g)	21.900 ± 0.13

Based on the FTIR spectrum in Fig. 1, MESSP showed similar chemical functional groups as other natural fillers from plant fibers (Khalil *et al.* 2001; Sgriccia *et al*. 2008), kenaf (Nacos *et al*. 2006; Jonoobi *et al*. 2009; Abdrahman and Zainudin 2011; Viet *et al*. 2012), wheat straw and soy hulls (Alemdar and Sain 2008), hemp fibers (Troedec *et al*. 2008), cellulose fibers (Silva *et al*. 2008), and wood fibers (Bodirlau and Teaca 2009). As illustrated in Fig. 1, the main absorption bands and peaks of MESSP were observed at 3305 cm^{-1}, 2918 cm^{-1}, 1726 cm^{-1}, 1611 cm^{-1}, 1510 cm^{-1}, 1439 cm^{-1}, 1362 cm^{-1}, 1235 cm^{-1}, and 1032 cm^{-1}. The characteristic band that appeared in the range of 3400 cm^{-1} to 3200 cm^{-1} was attributed to the stretching of O-H groups, which corresponded to the peak located at 3305 cm^{-1} in MESSP. The band in the range of 3000 cm^{-1} to 2800 cm^{-1} corresponded to C-H stretching in methyl and methylene groups, which appeared at 2918 cm^{-1} in MESSP (Khalil *et al*. 2001; Bodirlau and Teaca 2009; Jonoobi *et al*. 2009). The absorption peak in the region of 1730 cm^{-1} to1740 cm^{-1} was due to C=O

stretching in the carbonyl groups (Bodirlau and Teaca 2009; Abdrahman and Zainudin 2011), C=O stretching in the acetyl groups of hemicelluloses, or ester linkages in the carboxylic groups (Alemdar and Sain 2008; Jonoobi *et al*. 2009), and the absorption peak was detected at 1726 cm^{-1} in MESSP.

Furthermore, the peak corresponding to the absorbed moisture by the cellulose appeared at 1611 cm^{-1} in MESSP (Troedec *et al*. 2008; Jonoobi *et al*. 2009). The absorption peak at 1510cm^{-1} was caused by the vibration of aromatic skeletal (C=C aromatic) of lignins in MESSP (Troedec *et al*. 2008). A characteristic peak at 1439 cm^{-1} corresponded to CH_2 symmetric bending of cellulose (Sgriccia *et al*. 2008; Bodirlau and Teaca 2009; Abdrahman and Zainudin 2011), the peak at 1362 cm^{-1} was due to bending vibration of C-H of cellulose and hemicelluloses (Bodirlau and Teaca 2009), and the peak at 1235 cm^{-1} corresponded to the O-H phenolic (Bodirlau and Teaca 2009) or C-O stretching of aryl groups in lignin (Troedec *et al*. 2008). Finally, the peak at 1032 cm^{-1} was due to stretching of C-O of alcohol (primary and secondary), O-H, or aliphatic ethers (Nacos *et al*. 2006).

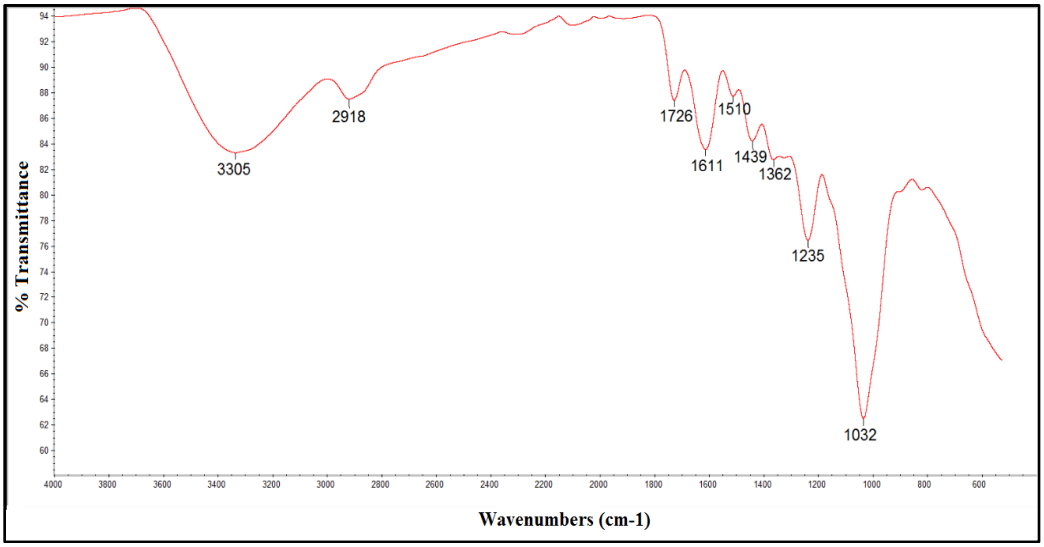

Fig. 1. FTIR spectra for MESSP

Figure 2 shows the percentage weight loss of MESSP due to decomposition *versus* temperature. This analysis confirmed that MESSP possessed moderate thermal stability. Approximately 70% of the MESSP decomposed upon heating from 30 °C to 600 °C. The temperature of maximum weight loss rate was 365 °C.

There were two stages of thermal decomposition behavior. The first stage of decomposition occurred at approximately 70 °C, and approximately 7.6% weight loss was recorded. This was due to volatilization of water or moisture in MESSP. This result is similar to other reports on the evaporation of absorbed moisture from natural fillers at 70 °C to 100 °C (Guan *et al*. 2013).

The second stage of decomposition occurred from 340 °C to 550 °C due to the decomposition of organic components such as cellulose, hemicellulose, and lignin; approximately 76% of the mass in the MESSP was decomposed. However, above 550 °C, the weight loss became constant. This result suggested that MESSP can withstand high temperatures above 550 °C and can be processed at higher temperatures with a wide range of polymers.

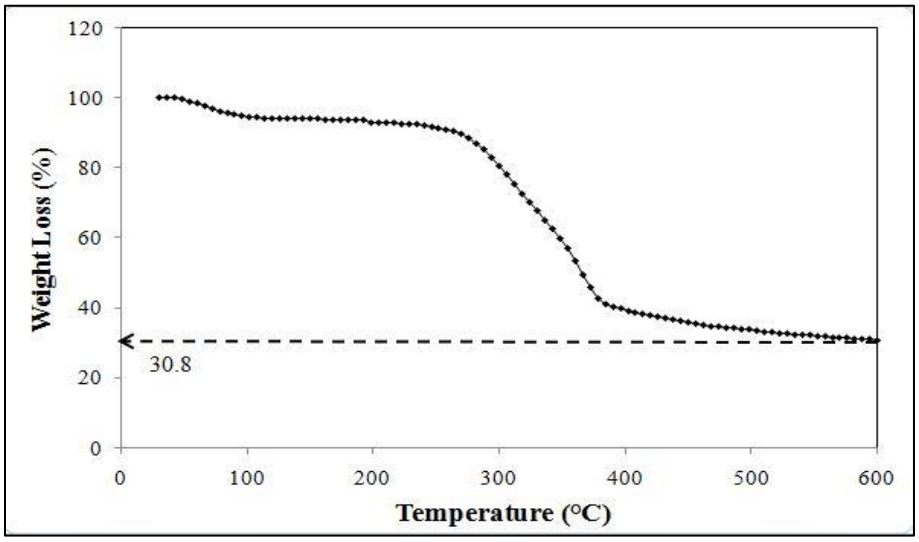

Fig. 2. Percentage weight loss of MESSP

Figure 3 shows the SEM micrographs of MESSP particles. MESSP particles were irregular in shape and size, and they appeared as individual particles or loosely bound aggregates at 500x magnification (Fig. 3a). The surface of MESSP particles was flat and smooth, which indicated high modulus in the MESSP particles. There were no distinctive pores or cracks can be observed on the surface of MESSP. A study by Kovacik (1999) reported on the low modulus of particles with the presence of porosity which can be related to the low mechanical stability of the solids with the presence of pores. Thus, it was expected that the flat surface of MESSP can possibly allow more PP chains to physically adhere to the surface of MESSP, which could induce stronger interfacial adhesion between PP and MESSP. This feature could subsequently enhance the properties of PP/MESSP composites.

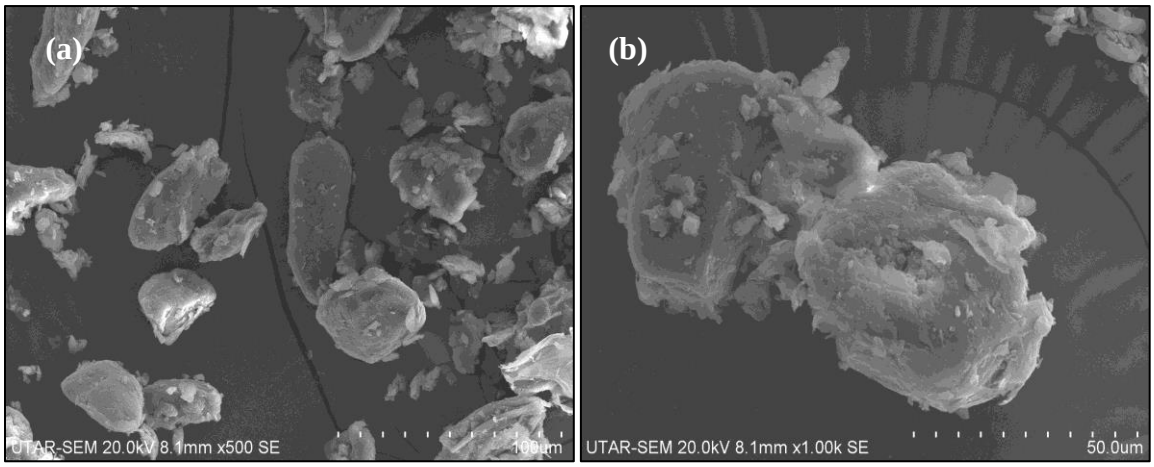

Fig. 3. Micrograph of MESSP at (a) 500x magnification (b) 1000x magnification

Processability of PP/MESSP Composites

The processability of polymer composites can be evaluated from the processing torque and temperature characteristics. The torque values reveal the processing properties

such as processability and stiffness of the composites. Thermal characteristics such as melting temperature, crystallization temperature, and degree of crystallinity indicate the influence of filler addition on the processing parameters of composites as compared to the neat polymers (Aho 2011). During melt mixing, the PP resins were melted by high temperature plates and mixed with the MESSP to produce homogeneous compounds. The shearing actions between PP resins tend to produce a high frictional force, which resulted in high shear stress and higher processing torque values. The loading torque, which was the initial torque, produced upon polymer discharge was highly dependent on the amount of PP resin. The stabilization torque indicated the final torque produced upon formation of the homogeneous mixture. A lower stabilization torque indicates easy processing, low stiffness of the compounds, and homogeneous dispersion of filler in the polymer matrix (Viet *et al*. 2012).

Figure 4 represents the torque-time profile of PP/MESSP composites, whereas Table 3 shows the loading and stabilization torque values produced when increasing the MESSP loading. Based on Fig. 4 and Table 3, the loading torque gradually decreased, whereas the stabilization torques of the PP was increased slightly with increasing MESSP loading. Reduction in the loading torque was due to the reduction in the amount of PP resins with increasing the MESSP loading. Low melt viscosity was produced with reducing the amount of PP and resulted in low shear, which reflects the low loading torque values. In contrast, the stabilization torques of PP/MESSP composites was increased slightly with increasing MESSP loading. Stabilization torque of composites depends mainly on the dispersion of the filler particles to produce a homogeneous mixture (Viet *et al*. 2012). Thus with increasing MESSP loading, more shear force is required to homogeneously disperse MESSP in PP which can be related to the increased stabilization torque values. Figure 4 also confirms that the MESSP particles were homogeneously dispersed in the PP matrix, which can be observed from the constant torque values being achieved at the stabilization region. Thus, the PP/MESSP composites with similar stiffness as the neat PP can be processed through the melt mixing of PP and MESSP using a Brabender internal mixer without needing to change the processing temperature, mixing time, and mixing speed (Pang *et al.* 2015).

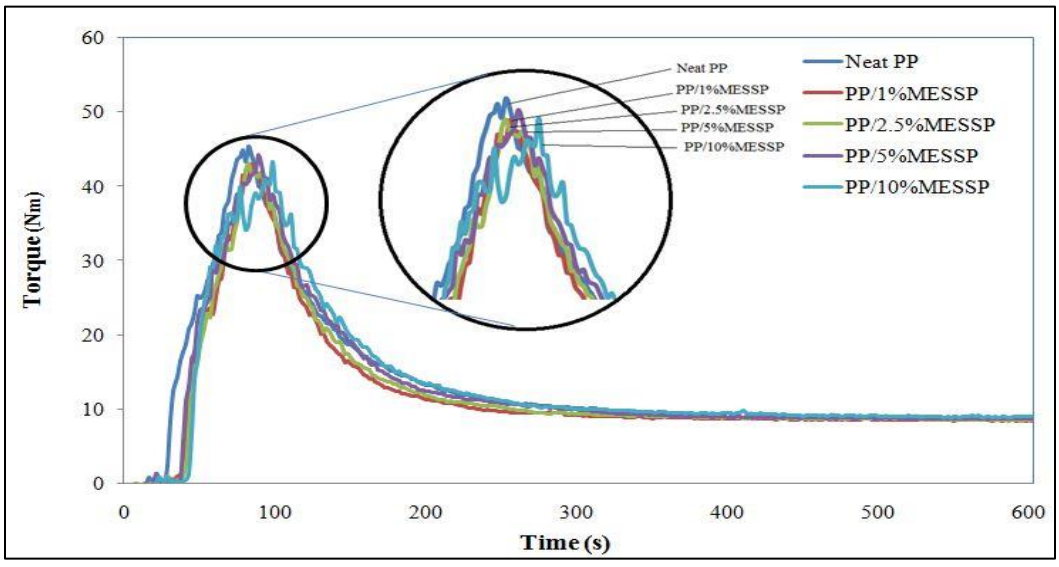

Fig. 4. Torque-time profiles of PP/MESSP composites

Table 3. Processing Torque Values of PP/MESSP Composites

Parameters	MESSP Loading (wt.%)				
	0	1	2.5	5	10
Loading Torque (Nm)	45.5 ± 1.1	44.1 ± 1.2	43.6 ± 0.8	43.3 ± 1.2	43.3 ± 1.3
Stabilization Torque (Nm)	8.5 ± 0.16	8.5 ± 0.13	8.6 ± 0.18	8.8 ± 0.15	8.9 ± 0.16

Table 4 illustrates the DSC results obtained for the neat PP and PP/MESSP composites when increasing the MESSP loading at the isothermal condition. The melting temperature (T_m) and crystallization temperature (T_c) of PP were marginally affected when the MESSP loading was increased. Notably, at 1 wt.% MESSP loading, the composite T_m and T_c increased slightly, whereas further increasing the MESSP loading above 1 wt.% resulted in a small decrease in the T_m and T_c. The enthalpy of melting and the degree of crystallinity of the PP also showed similar trends as depicted in Table 4. Enthalpy of melting and degree of crystallinity were increased slightly with the initial addition of 1 wt.% MESSP. However, the values were both decreased marginally with further increases in MESSP loading above 1 wt.%.

Similar observations were reported by Papageorgiou *et al.* (2014) on the addition of silica nanotube (SiNT) in polybutylene succinate. Papageorgiou *et al.* (2014) reported that T_c increases with increasing SiNT content, which is due to the nucleation activity of SiNT that increases the rate of crystallization. However, an earlier study by Papageorgiou *et al.* (2005) reported that the T_c and crystallization rate decreased when the silica loading increased due to the formation of aggregates, which inhibited the formation of crystalline structures and lowered the rate of crystallization and T_c. Thus, MESSP acts as a nucleating agent at a low loading of 1 wt.% and tend to induce crystallization at lower temperatures. Thus, there was a slight increase in the T_m and T_c, which contributed to a higher melting enthalpy and a higher degree of crystallinity in the PP/MESSP composites as when compared to neat PP.

However, when the MESSP loading increased above 1 wt.%, the segmental mobility of the PP chains reduced due to stiffening in the PP network, which gradually hinders the rate of crystallization. Hence, the T_m and T_c decreased marginally and resulted in the enthalpy of melting and degree of crystallinity to gradually decrease. Besides, the SEM morphology also confirmed the presence of MESSP agglomerates at 10 wt.% loading, which could inhibit the crystallization rate and result in a reduction in the degree of crystallinity similar to Papageorgiou *et al.* (2005).

Table 4. Thermal Characteristics of PP/MESSP Composites

Parameters	**MESSP loading (wt.%)**				
	0%	**1%**	**2.5%**	**5%**	**10%**
Melting Temperature, T_m (ºC)	172.75	173.11	172.57	172.41	172.26
Crystallization Temperature, T_c (ºC)	125.64	126.09	125.63	125.25	125.10
Enthalpy of Melting, ΔH_m (J/g)	89.98	92.67	89.17	84.60	79.59
Degree of Crystallinity, X^m_c (%)	43.47	45.22	43.19	43.02	42.72

The overall analysis of the processing torque and DSC revealed that addition of MESSP did not drastically change the processability of PP. The loading and stabilization torque of PP/MESSP composites were all comparable to the processing torque of the neat PP. This shows that addition of MESSP did not change the melt viscosity and rheological

behavior of PP. Besides, the DSC analysis also confirmed that MESSP addition did not affect the T_m, T_c, enthalpy of melting, and degree of crystallinity in PP. Hence, PP/MESSP composites can be developed with similar processing conditions used in neat PP, while retaining the degree of crystallinity with the addition of MESSP of up to 10 wt.%.

Water Absorption

MESSP is hydrophilic in nature and contains hydroxyl groups as shown through the FTIR analysis. The presence of hydroxyl groups may lead to moisture absorption by the PP/MESSP composites. Thus, water absorption measurement was carried out to determine the water absorption capacity of PP/MESSP composites as compared to neat PP. According to Acevedo *et al*. (2016), the water absorption capability of natural fillers depended on several factors mainly the particle size, surface area exposed, porosity, and the presence of hydroxyl group within the chemical structure.

Based on Fig. 5, the percentage of water absorption was increased slightly with the addition of MESSP, which showed a gradual increasing trend with increasing the MESSP loading. This result is similar to Demir *et al.* (2006), which showed an increase in the water absorption of the luffa fiber filled PP composites. According to Demir *et al.* (2006), the amount of water absorbed by the composites increased with the increasing filler loading due to the formation of hydrogen bonding between the hydroxyl groups on the cellulose structure of natural filler and water molecules. This study proves that increasing water absorption by PP/MESSP with increasing MESSP loading is due to the presence of hydroxyl groups in MESSP. However, the percentage water absorption of PP/MESSP composites was only increased by approximately 0.07% when 10 wt.% MESSP was added into PP which is very low.

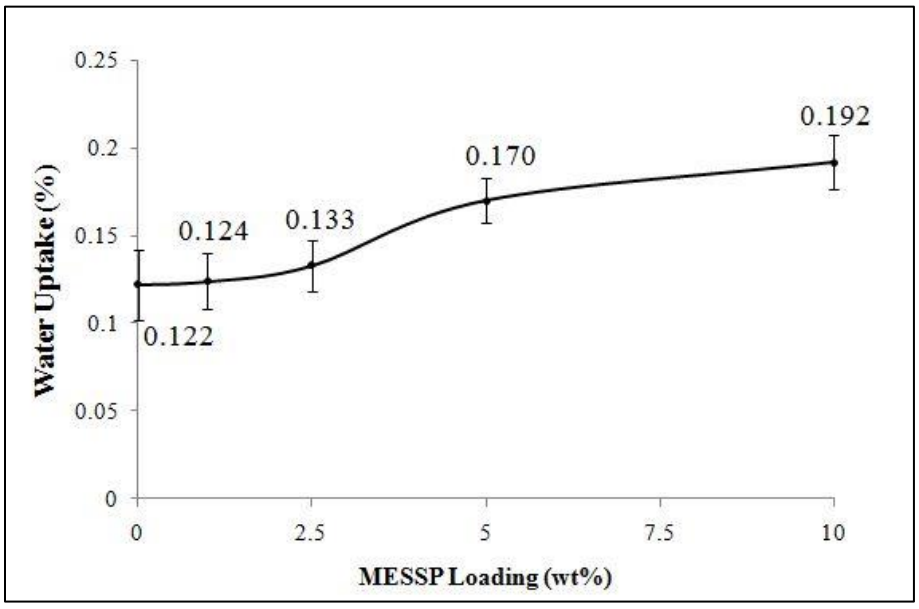

Fig. 5. Percentage water absorption of PP/MESSP composites

Tensile Properties of PP/MESSP Composites

Figure 6 depicts the effect of increasing MESSP loading on the tensile strength of PP/MESSP composites. Tensile strength of PP/MESSP composites increased gradually

with the increasing of the MESSP loading to 5 wt.% and reduced slightly at a high MESSP loading of 10 wt.%. The tensile strength of a composite material depends strongly on several factors such as the particle size of the filler, filler/matrix ratio, filler dispersion, and the interfacial adhesion between the filler and matrix (Fu *et al*. 2008). SEM morphological observation of the tensile fractured sample revealed that MESSP particles were well dispersed in the PP matrix and showed good interfacial adhesion, which could have been the dominant factor contributing towards the increasing tensile strength of PP/MESSP composites as compared to neat PP. However, agglomeration of MESSP was observed at high MESSP loading of 10 wt.%, which was the reason for the slight reduction in the tensile strength. This observation was further discussed under morphological observations.

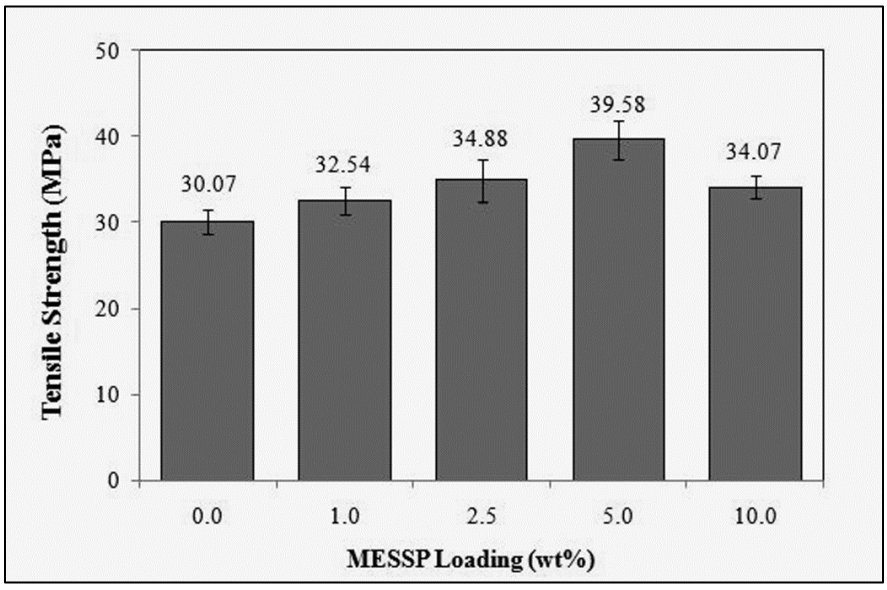

Fig. 6. Variation in tensile strength of PP/MESSP composites

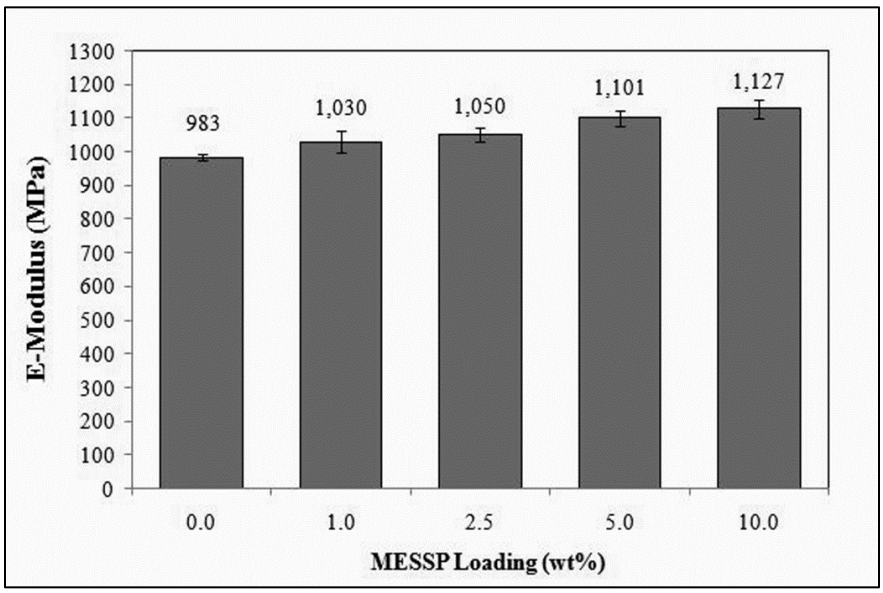

Fig. 7. Variation in E-Modulus of PP/MESSP composites

Figure 7 illustrates the effect of MESSP addition on the E-modulus of PP/MESSP composites at different MESSP loading. E-modulus or tensile modulus refers to the stiffness of composites and its resistance to fracture when stress is applied (Fu *et al*. 2008). According to Pang *et al.* (2015) higher E-modulus values indicates high stiffness and rigidity of PP/kenaf composites. The stiffness of PP/MESSP composites was enhanced with the inclusion of MESSP in PP matrix. The enhancement of E-modulus can be related to the reduction in segmental mobility of PP chains due to restriction of the MESSP particles. Furthermore, good interfacial adhesion between MESSP and PP further reduced the mobility of PP chains. A similar observation was reported by Bakar *et al.* (2015) on the enhancement of tensile modulus of PVC/EVA blends with the incorporation of kenaf fiber which and was due to the reduction in segmental mobility of PVC/EVA network in the presence of kenaf fibers.

Figure 8 shows the results for the elongation at the break of PP/MESSP composites with the increasing of MESSP loading. In contrast to the E-modulus values, elongation at break was gradually reduced with increasing MESSP loading. Due to the increasing MESSP content in the composite, the mobility of PP chain was inhibited, causing low deformability of the composites. The high rigidity of composites due to the high filler loading and agglomeration of fillers, which act as the rigid part in polymers, may further cause the reduction in elongation at break. Similar observations were reported by Pang *et al.*(2015) on the reduction of the elongation at break with increasing the kenaf fiber loading due to the increased rigidity of the composite.

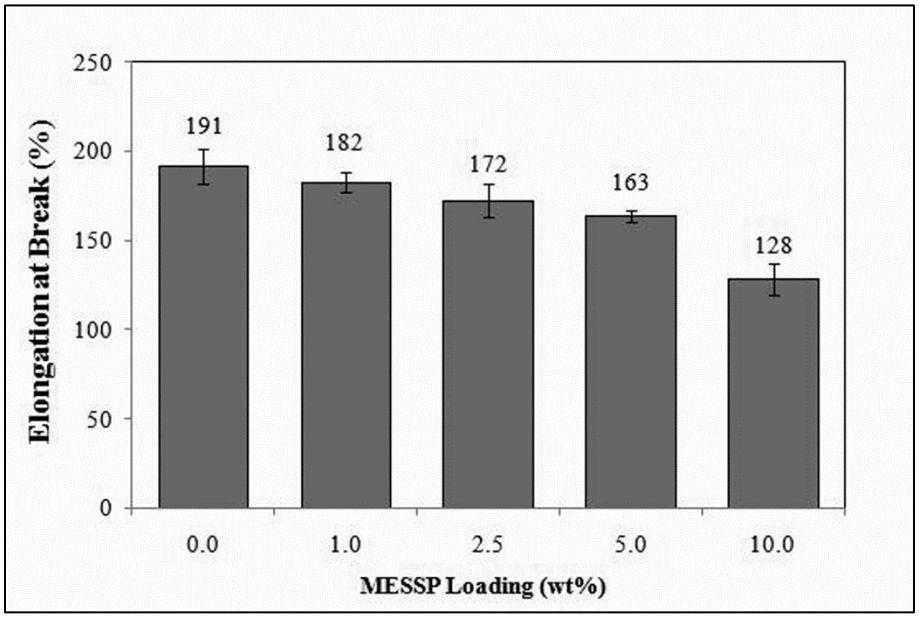

Fig. 8. Variation in elongation at break of PP/MESSP composites

SEM Morphological Observation

Figure 9 shows the SEM micrographs of the tensile fractured surfaces of PP/MESSP composites at different MESSP loadings (1000x magnification). The fractured surface of neat PP as shown in Fig. 9a, indicates the roughest surface with fibrous structure as compared to the surfaces of PP/MESSP composites. Based on the surface characteristics of neat PP, it was revealed that neat PP had the highest matrix tearing and thus demonstrates the highest deformability. This morphology confirms the

highest elongation at break of neat PP as compared to PP/MESSP composites. However, the surface roughness of the PP was reduced with the addition of MESSP, as can be seen from Fig. 9b to Fig. 9e. This observation also confirms that addition of MESSP increases the stiffness of the composites, which made the fracture surface to be smoother. This observation is in agreement with the tensile results, which indicate increasing E-modulus and reduction of elongation at break of PP/MESSP composites with increasing MESSP loading, respectively.

Furthermore, based on Fig. 9 the MESSP particles were well dispersed in the PP matrix and had a good interfacial adhesion with PP. MESSP particles were observed to be well embedded and attached to the fracture surface, which indicated good interfacial adhesion. Fig. 8d represents the fractured surface of PP/MESSP composite containing 5 wt.% MESSP showed the best surface morphology with good adhesion between MESSP and PP as well as good matrix tearing as compared to other PP/MESSP composites. Besides, it was also revealed from Fig. 9e that MESSP particles tend to agglomerate in the PP matrix and resulted in poor interfacial adhesion. This can be evidenced from the presence of wide gap at the interface of MESSP agglomerate and PP matrix. According to Ismail and Mathialagan (2011), agglomerate particles of filler tend to act as stress concentration point and resulted in an uneven stress distribution from the matrix to the filler which lowers the tensile strength and mechanical properties of polymer composites. Hence, this observation supports the reduction in tensile strength of PP/MESSP composite at 10 wt.% MESSP loading, which was due to the agglomeration of the MESSP particles.

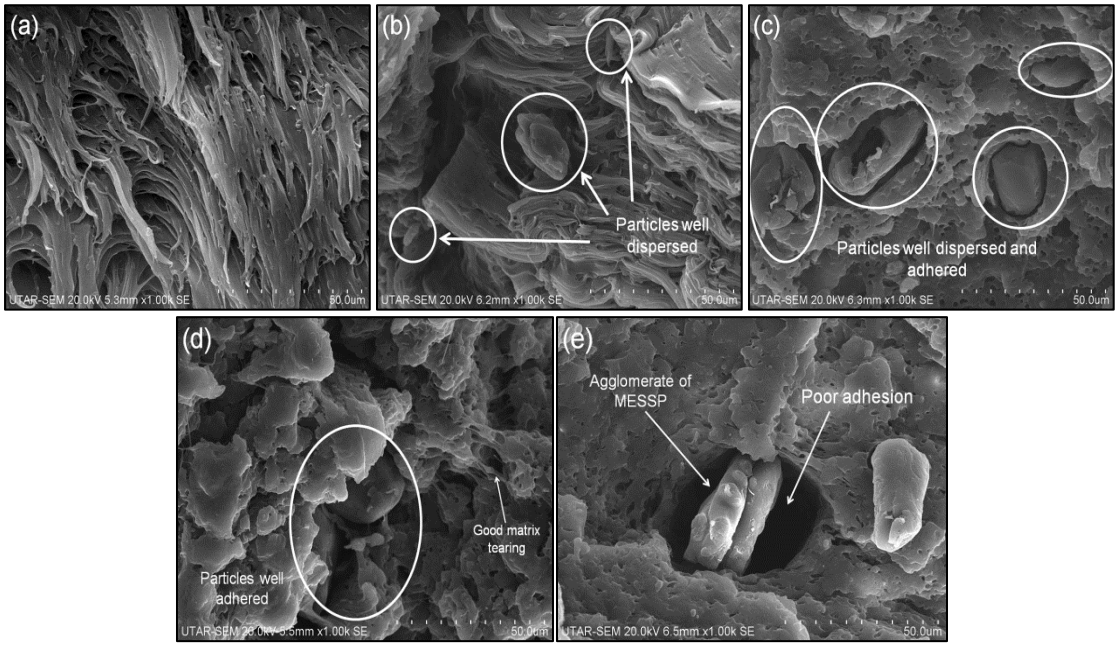

Fig. 9. Comparison of surface morphology of PP/MESSP composites; (a) neat PP, (b) PP/MESSP-1%, (c) PP/MESSP-2.5%, (d) PP/MESSP-5% and (e) PP/MESSP-10% (1000x magnification)

CONCLUSIONS

1. From the results, MESSP was characterized and introduced as a new bio-filler in the PP matrix to produce PP/MESSP biocomposites. MESSP particles exhibited irregular particle shape and size with smooth and flat surface morphology and was presented either as an individual particle or as a loosely bound aggregate structure when viewed under a SEM. The particle size analysis revealed that the MESSP had a narrow particle size distribution with a mean diameter of 0.583 µm and a specific surface area of 21.9 m^2/g. Meanwhile, the thermal stability study showed that the MESSP had a moderate thermal decomposition temperature of 365 °C.
2. An addition of MESSP up to 10 wt.% did not affect the processability of the PP matrix as revealed from the comparable processing torque values, melting temperature, crystallization temperature, enthalpy of melting, and degree of crystallinity.
3. Moreover, MESSP showed great potential to be used as a new bio-filler in the PP matrix as depicted from the enhanced tensile strength, E-modulus, and comparable water absorption percentage of PP/MESSP composites as compared to neat PP. However, the elongation at break was compromised with increasing the MESSP loading.
4. The SEM morphological observation revealed that MESSP particles were well dispersed in the PP matrix and showed good interfacial adhesion up to 5 wt.% MESSP loading. However, the agglomeration of MESSP can be observed above 5 wt.% MESSP loading, which was responsible for the slight reduction in the tensile strength of the PP/MESSP composites.
5. PP/MESSP composites can be used in many applications that requires medium tensile strength, water absorption, and processability as similar to PP such as the interior parts of car, car dashboards and door panels, housewares, furniture, consumer products, and rigid packaging.

ACKNOWLEDGMENTS

The authors thank University Tunku Abdul Rahman for providing all the necessary equipment to conduct this research.

REFERENCES CITED

Abdrahman, M. F., and Zainudin, E. S. (2011). "Properties of kenaf filled unplasticized polyvinyl chloride composites," *Key Engineering Materials* 471-472, 507-512. DOI: 10.4028/www.scientific.net/KEM.471-472.507.

Acevedo, M., Tapia, A., Correa, J., Ricardo, R., and Realpe, A. (2016). "Characterization of recycled polypropylene composite material reinforced with wood flour using SEPS-g-MAH as coupling agent," *International Journal of Engineering and Technology* 8(2), 1397-1405.

Aho, J. (2011). *Rheological Characterization of Polymer Melts in Shear and Extension:*

Measurement Reliability and Data for Practical Processing, Ph.D. Dissertation, Tampere University of Technology, Hervanta, Tampere, Finland.

Alemdar, A., and Sain, M. (2008). "Isolation and characterization of nanofibers from agricultural residues - Wheat straw and soy hulls," *Bioresource Technology* 99(6), 1664-1671. DOI: 10.1016/j.biortech.2007.04.029.

Alomayri, T., Assaedi, H., Shaikh, F. U. A., and Low, I. M. (2014). "Effect of water absorption on the mechanical properties of cotton fabric reinforced geopolymer composites," *Journal of Asian Ceramic Societies* 2(3), 223-230. DOI: 10.1016/j.jascer.2014.05.005.

ASTM D638-14 (2014). "Tensile properties of plastics," ASTM International, West Conshohocken, PA.

ASTM D570-98 (2010). "Water absorption of plastics," ASTM International, West Conshohocken, PA.

Bakar, N. A., Chee, C. Y., Abdullah, L. C., Ratnam, C. T., and Ibrahim, N. A. (2015). "Thermal and dynamic mechanical properties of grafted kenaf filled polyvinyl chloride and ethylenevinylacetate composites," *Materials and Design* 65, 204-211. DOI: 10.1016/j.matdes.2014.09.027.

Baliga, M. S., Pai, R. J., Bhat, H. P., Palatty, P. L., and Boloor, R. (2011). "Chemistry and medicinal properties of the Bakul (*Mimusops elengi* Linn) - A review," *Food Research International* 44(7), 1823-1829. DOI: 10.1016/j.foodres.2011.01.063.

Bjørk, R., Tikare, V., Frandsen, H. L., and Pryds, N. (2012). "The effect of particle size distributions on the microstructural evolution during sintering," *Journal of the American Ceramic Society* 96(1), 103-110. DOI: 10.1111/jace.12100.

Bodirlau, R., and Teaca, C.A. (2009). "Fourier transform infrared spectroscopy and thermal analysis of lignocelluloses fillers treated with organic anhydrides," *Romanian Journal of Physics* 54(1-2), 93-104.

Boonyuen, C., Wangkarn, S., Suntornwat, O., and Chaisuksant, R. (2009). "Antioxidant capacity and phenolic content of *Mimusops elengi* fruit extract," *Kasetsart Journal (Natural Science)* 43(1), 21-27.

Bora, P., Konwar, L. J., Boro, J., Phukan, M. M., Deka, D., and Konwar, B. K. (2014). "Hybrid biofuels from non-edible oils - A comparative standpoint with corresponding biodiesel," *Applied Energy* 135(15), 450-460. DOI: 10.1016/j.apenergy.2014.08.114.

Demir, H., Atikler, U., Balköse, D., and Tıhmınlıoğlu, F. (2006). "The effect of fiber surface treatments on the tensile and water sorption properties of polypropylene - luffa fiber composites," *Composites Part A: Applied Science and Manufacturing* 37(3), 447-456. DOI: 10.1016/j.compositesa.2005.05.036.

Dutta, K., and Deka, D. (2014). "Physicochemical characteristics and triglyceride composition of *Mimusops elengi* seed oil," *Advances in Applied Science Research* 5(1), 65-73.

Fakhrul, T., and Islam, M. (2013). "Degradation behavior of natural fiber reinforced polymer matrix composites," *Procedia Engineering* 56, 795-800. DOI: 10.1016/j.proeng.2013.03.198.

Faruk, O., Bledzki, A., Fink, H., and Sain, M. (2012). "Biocomposites reinforced with natural fibers: 2000-2010," *Progress in Polymer Science* 37(11), 1552-1596. DOI: 10.1016/j.progpolymsci.2012.04.003.

Fu, S. Y., Feng, X. Q., Lauke, B., and Mai, Y. W. (2008). "Effects of particle size, particle/matrix interface adhesion and particle loading on mechanical properties of particulate - polymer composites," *Composites Part B: Engineering* 39(6), 933-961.

DOI: 10.1016/j.compositesb.2008.01.002.

Gami, B., Pathak, S., and Parabia, M. (2012). "Ethnobotanical, phytochemical and pharmacological review of *Mimusops elengi* Linn," *Asian Pacific Journal of Tropical Biomedicine* 2(9), 743-748. DOI:10.1016/s2221-1691(12)60221-4.

Guan, B. T. H., Latif, P. A., and Yap, T. Y. H. (2013). "Physical preparation of activated carbon from sugarcane bagasse and corn husk and its physical and chemical characteristics," *International Journal of Engineering Research and Science & Technol*ogy 2(3), 1-14.

Hamad, K., Kaseem, M., and Deri, F. (2013). "Recycling of waste from polymer materials: An overview of the recent works," *Polymer Degradation and Stability* 98(12), 2801-2812. DOI: 10.1016/j.polymdegradstab.2013.09.025.

Ismail, H., and Mathialagan, M. (2011). "Curing characteristics, morphological, tensile, and thermal properties of bentonite-filled ethylene-propylene-diene monomer (EPDM) composites," *Polymer-Plastics Technology and Engineering* 50(14), 1421-1428. DOI: 10.1080/03602559.2011.584244.

Jonoobi, M., Harun, J., Shakeri, A., Misra, M., and Oksman, K. (2009). "Chemical composition, crystallinity, and thermal degradation of bleached and unbleached kenaf bast (*Hibiscus cannabinus*) pulp and nanofibers," *BioResources* 4(2), 626-639.

Kadam, P. V., Yadav, K. N., Deoda, R. S., Shivatare, R. S., and Patil, M. J. (2012). "*Mimusops elengi* – A review on ethnobotany, phytochemical, and pharmacological profile," *Journal of Pharmacognosy and Phytochemistry* 1(3), 64-74.

Khalil, H. P. S. A., Ismail, H., Rozman, H. D., and Ahmad, M. N. (2001). "The effect of acetylation on interfacial shear strength between plant fiber and various matrices," *European Polymer Journal* 37(5), 1037-1045. DOI:10.1016/S0014-3057(00)00199-3.

Kovacik, J. (1999). "Correlation between Young's modulus and porosity in porous materials," *Journal of Materials Science Letters* 18(13), 1007-1010. DOI: 10.1023/A:1006669914946.

Lim, T. K. (2013). "*Mimusops elengi*," in: *Edible Medicinal and Non-Medicinal Plants(Vol. 6 Fruits*), Springer, Dordrecht, Netherlands, pp.119-128. DOI: 10.1007/978-94-007-5628-1.

Lu, X., and Xu, G. (1997). "Thermally conductive polymer composites for electronic packaging," *Journal of Applied Polymer Science* 65(13), 2733-2738. DOI: 10.1002/(SICI)1097-4628(19970926)65:13<2733::AID-APP15>3.0.CO;2-Y.

Mitra, R. (1981). "Bakula, a reputed drug of ayurveda, its history, uses in Indian medicine," *Indian Journal of History of Science* 16(2), 169-180.

Nacos, M. K., Katapodis, P., Pappas, C., Daferera, D., Tarantilis, P. A., Christakopoulos, P., and Polissiou, M. (2006). "Kenaf xylan - A source of biologically active acidic oligosaccharides," *Carbohydrate Polymers* 66(1), 126-134. DOI: 10.1016/j.carbpol.2006.02.032.

Pang, A., Ismail, H., and Bakar, A. A. (2015). "Effects of kenaf loading on processability and properties of linear low-density polyethylene/poly(vinylalcohol)/kenaf composites," *BioResources* 10(4), 7302-7314.

Papageorgiou, G. Z., Achilias, D. S., Bikiaris, D. N., and Karayannidis, G. P. (2005). "Crystallization kinetics and nucleation activity of filler in polypropylene/surface-treated SiO_2 nanocomposites," *Thermochimica Acta* 427(1-2), 117-128. DOI: 10.1016/j.tca.2004.09.001.

Papageorgiou, G. Z., Papageorgiou, D. G., Chrissafis, K., Bikiaris, D., Will, J., Hoppe, A., Roether, J. A., and Boccaccini, A. R. (2014). "Crystallization and melting

behavior of poly(butylene succinate) nanocomposites containing silica-nanotubes and strontium hydroxyapatite nanorods," *Industrial and Engineering Chemistry Research* 53(2), 678-692. DOI: 10.1021/ie403238u.

Prnewswire (2015). *Global Polymer Industry 2015-2020: Trend, Profit, and Forecast Analysis (Report ID: 2788885*), (http://www.prnewswire.com/news-releases/global-polymer-industry-2015-2020-trend-profit-and-forecast-analysis-300131254.html), Accessed 10 July 2017.

Sathishkumar, T., Naveen, J., and Satheeshkumar, S. (2014). "Hybrid fiber reinforced polymer composites - A review," *Journal of Reinforced Plastics and Composites* 33(5), 454-471. DOI: 10.1177/0731684413516393.

Sgriccia, N., Hawley, M. C., and Misra, M. (2008). "Characterization of natural fiber surfaces and natural fiber composites," *Composites Part A: Applied Science and Manufacturing* 39(10), 1632-1637. DOI: 10.1016/j.compositesa.2008.07.007.

Shibata, S., Cao, Y., and Fukumoto, I. (2006). "Lightweight laminate composites made from kenaf and polypropylene fibres," *Polymer Testing* 25(2), 142-148. DOI: 10.1016/j.polymertesting.2005.11.007.

Silva, M. C., Lopes, O. R., Colodette, J. L., Porto, A. O., Rieumont, J., Chaussy, D., Belgacem, M. N., and Silva, G. G. (2008). "Characterization of three non-product materials from a bleached eucalyptus kraft pulp mill, in view of valorising them as a source of cellulose fibres," *Industrial Crops and Products* 27(3), 288-295. DOI: 10.1016/j.indcrop.2007.11.005.

Stein, R. S. (2002). "Plastics can be good for the environment," *NEACT Journal* 21(1), 10-12.

Troedec, M. L., Sedan, D., Peyratout, C., Bonnet, J. P., Smith, A., Guinebretiere, R., Gloaguen, V., and Krausz, P. (2008). "Influence of various chemical treatments on the composition and structure of hemp fibres," *Composites Part A: Applied Science and Manufacturing* 39(3), 514-522. DOI: 10.1016/j.compositesa.2007.12.001.

Viet, C. X., Ismail, H., Rashid, A. A., and Takeichi, T. (2012). "Kenaf powder filled recycled high-density polyethylene/natural rubber biocomposites – The effect of filler content," *International Journal of Integrated Engineering* 4(1), 22-25.

Article submitted: August 29, 2017; Peer review completed: October 8, 2017; Revised version received: October 27, 2017; Published: November 17, 2017.
DOI: 10.15376/biores.13.1.272-289